A high step–up DC–DC converter with MPPT for PV application

María del Rosario Rivera-Espinosa*, Alfredo Y. Alejandre-López*, Jesús E. Pedraza-Barrón*,
Pedro Martín García-Vite* and Héctor R. Robles-Campos†.
*TECNM / Instituto Tecnológico de Ciudad Madero,
División de Estudios de Posgrado e Investigación, J. Rosas y J. Urueta, s/n,
Los Mangos, CP. 89440, Cd. Madero, Tams., México; tel:+52(833)215-85-44.
†Universidad Panamericana, Campus Guadalajara,
Facultad de Ingeniería, Zapopan, Jalisco CP. 45010, México.

***Abstract*—This paper exhibits the performance of a high step–up converter employed for maximum power extraction in a photovoltaic system. The proposed converter is conformed by a conventional boost followed by a diode-capacitor-based multiplier for increasing the nominal voltage gain of the boost converter, resulting in a lower duty cycle at the maximum power point. The main characteristics of the converters are analyzed in order to determine an optimal equivalent input impedance. Evaluation of the proposed converter using standard Perturb and Observe algorithm is carried out. Switching simulations evidence the good performance of the whole system under irradiance disturbances.**

I. Introduction

A photovoltaic (PV) panel has a unique operating point called the Maximum Power Point (MPP), at which the extraction of the available power is maximized, for given climatic conditions such as temperature and solar radiation [1].

The MPP depends not only on the climatic conditions but also on the PV panel manufacturing characteristics, that means every module might have a different MPP even in cells of the same type. Besides, this MPP moves in an unpredictable way. Even though, it is possible to obtain the current-voltage or I-V curve of the PV panel by means of experimental measurements in order to know the MPP location, it is necessary to use efficient techniques for tracking the MPP [1]. Algorithms for extracting the maximum power from the PV panel are called MPP trackers (MPPT). Thus, many MPPT algorithms have been developed in order to achieve maximum efficiency in operation [2], [3].

The PV panel curve can be experimentally obtained employing different methods; one of the simplest consists in connecting a variable resistor at the module terminals. Then, values of current and voltage are registered for different load conditions and finally the delivered power is computed [4]. Knowing the exact location of the MPP allows the implementation of straightforward algorithms based on the irradiance value, however an extra sensor is required which increases the total cost.

Fig. 1 contains a typical configuration of a PV system which is constituted by a power converter controlled by an MPPT algorithm feeding a fixed DC load R_{L}. The DC−DC converter, with a voltage gain of G_{v}, can emulate a variable resistance joining the PV module and the load. In terms of average values, the converter behaves as an impedance which depends on the value of R_{L} and duty cycle D [5]. In order to operate at the MPP the duty cycle generated by the MPPT algorithm needs to be adjusted, it is essential to select a suitable converter that allows reaching the MPP for a specific R_{L}, and therefore the converter input impedance seen by the module Z_{in}.

Basic converter topologies such as buck and boost are widely used for MPPT applications because of their simplicity. Nevertheless, there is a huge number of power converters well-reported in the literature [6] that enjoy their own advantages. An appropriate DC−DC converter selection will guarantee reaching all the range of optimal impedance values that the system requires throughout the sun hours. On the one hand, for low irradiance conditions, a high gain is desired in order to comply the load voltage level, thus several high gain converters have been proposed, however they usually present complex configuration and more than one single power transistor, which in turn increases the losses, whereas others are realized with a single power switch [7] overcoming this disadvantage. On the other hand, converters with gain flexibility like the conventional buck–boost are more adequate for PV applications since they offer an output voltage higher or lower than the input voltage [8]. However, the input current discontinuity deteriorates the MPPT algorithm performance [9]. It is desirable that the converter operates on the Continuous Conduction Mode (CCM) for high efficiency and continuous current through the inductor.

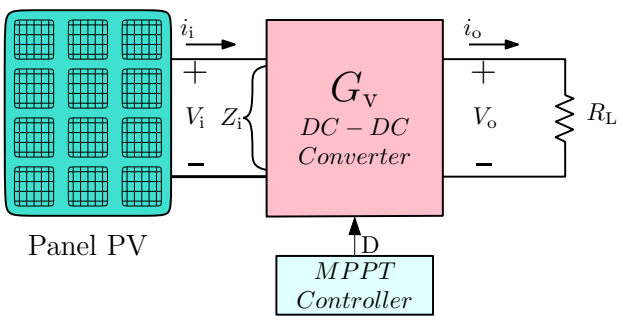

Fig. 1: Block diagram of the PV panel with MPPT control.

978-1-5386-0819-7/17/$31.00 ©2017 IEEE

This paper suggests the utilization of a boost DC−DC converter [10] with diode–capacitor multiplier controlled by an MPPT algorithm to interface a PV panel with a fixed load. The operation principles, analysis and the simulation results of the proposed converter are presented. Besides, guideline for power converter selection based on the input impedance characteristics are provided; also the utilization of a proposed DC−DC converter controlled by an MPPT algorithm is suggested and analyzed. A standard MPPT algorithm is taken as a reference in order to evaluate the proposed DC–DC converter.

The remaining of this paper is organized as follows: a brief review of the MPPT algorithms is carried out in Section II remarking the P & O technique which is taken as reference. Section III presents the relevance of the input impedance of various power converters. Section V the proposed converter is presented and analyzed in order to validate its effectiveness, then it is incorporated into the PV system as explained in VI. The theoretical analysis is validated via simulation and experimentation whose results are reported in Sections VII and VIII, respectively. Finally, conclusions close the paper.

II. MPPT Techniques

As mentioned before, there are several MPPT algorithms reported in the literature [9], some of them are very simple and easy to implement. Algorithms most frequently found in the literature are the Fractional Open Circuit Voltage [11], the Fractional Short Circuit Current [12] and the Perturb and Observe (P&O) [5], the latter has been accepted as a standard algorithm commonly used for comparison purposes. These algorithms present disadvantages like low accuracy and PV array model dependence. Others are fast with high degree of accuracy but possess complex structures, making these algorithms have high computational cost [13]. In general, the effectiveness of an algorithm is determined by some parameters like easiness of implementation, scheme complexity, number of required sensors, convergence speed and stability. Particularly, the P&O algorithm, shown in Fig. 2, is easy to design and implement, it does not need the PV panel model and it can be implemented either with analog or digital circuitry [5].

The P&O algorithm operates by changing the PV panel operating voltage and observing the power drawn from the PV source. The flowchart of the P&O method is presented in Fig. 2. The MPPT algorithm is continuously sampling the actual PV output voltage V_{k} and current I_{k}, then the power P_{k} is calculated. The differences between the power and voltage are obtained in dP and dV at the instant k and $k-1$. For a positive value of dV, if dP is positive, the step perturbation Δ_{D} should increase whereas if dP is negative, Δ_{D} must decrease. On the other hand, for a negative value of dV, Δ_{D} should change in an opposite way, as indicated in Fig. 2, [3]. After a several number of iteration steps the P&O algorithm will make the operating point oscillate around the MPP.

III. Converter Topologies

The equivalent input impedance (Z_{in}) of a power converter takes relevant importance in PV panel applications, since the ultimate objective of the converter is to manipulate the load "seen" by the source. In short, the converter acts as an interface between the load resistor which consumes usefully the energy and the PV panel. Table I summarizes ideal voltages and currents relationships of conventional power converters along with the proposed high step–up power converter. The input characteristic Z_{in} of each converter is also provided. The load value R_{L} depends on the particular application, however the equivalent impedance can be modified properly by the power converter, thus components selection is very important in the design process. Moreover, it is worth noting that R_{L} determines the range of Z_{in} needed to achieve the MPP and the range of duty cycles in which the converter will operate.

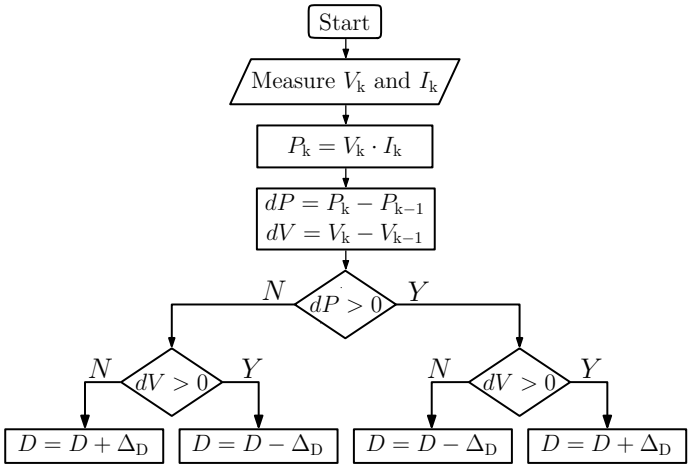

Fig. 2: Flowchart of P&O algorithm.

TABLE I: Converter parameters.

	Parameter		
Converter	$\frac{V_{\mathrm{o}}}{V_{\mathrm{i}}}$	$\frac{I_{\mathrm{o}}}{I_{\mathrm{i}}}$	Z_{in}
buck	D	$\frac{1}{D}$	$\frac{R_{\mathrm{L}}}{D^2}$
boost	$\frac{1}{1-D}$	$1-D$	$(1-D)^2 R_{\mathrm{L}}$
buck–boost	$\frac{-D}{1-D}$	$1-D$	$\frac{(1-D)^2}{D^2} R_{\mathrm{L}}$
High step–up	$\frac{1+D}{1-D}$	$\frac{1-D}{1+D}$	$\frac{(1-D)^2}{(1+D)^2} R_{\mathrm{L}}$

For a certain load, the PV panel "sees" an input impedance as plotted in the Fig. 3. And the most remarkable characteristics are the following: (*i*) converters with boost capability have a $Z_{\mathrm{in}} < R_{\mathrm{L}}$ condition, (*ii*) for the buck converter the characteristic is that $Z_{\mathrm{in}} > R_{\mathrm{L}}$, and (*iii*) the buck–boost converters can have an input impedance in a wider range, including lower or greater values of R_{L}.

It is important to note that Z_{in} decreases while the value of D rises as Fig. 3 shows.

The advantage of using the high step–up converter is that the

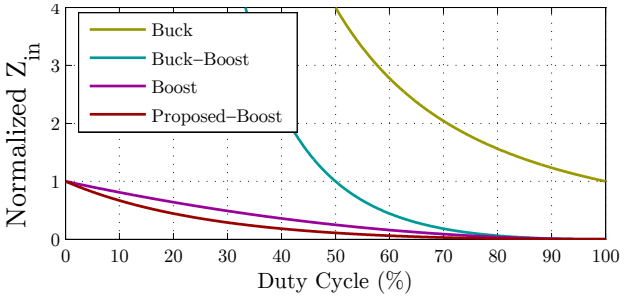

Fig. 3: Equivalent input impedance of various power converters.

PV panel is always loaded with a lower impedance in spite of possessing high voltage gain. As a result, the maximum extracted power can be achieved with a relatively low duty cycle which is desirable given the fact that it keeps the losses low.

IV. Applications of the MPPT algorithm

Two different realizations of the MPPT algorithm for PV systems can be accomplished. The utilization of a DC/AC converter in order to transform the DC power from the PV module to AC power is used in systems connected to the utility grid. However, this study is not considered in this work. Stand–alone PV systems are commonly used in low–power applications. An energy storage device, such as a battery, is necessary. The simplest way of integrating a battery with a PV panel is the direct parallel connection. Nevertheless, the battery tends to control the PV voltage and does not allow operating in the MPP. Moreover, this condition reduces the efficiency of the system and it is not possible to regulate the battery power [14]. For that reason, it is necessary to connect a DC–DC converter between the PV panel and the battery.

Battery charger systems are widely used in stand–alone PV systems, as presented in [15] with a novel battery charging regulation system. It consists of a buck converter controlled by an MPPT technique. The increase of the battery lifetime and the better exploitation of the PV source are the advantages of this method. Similarly in [16] an MPPT algorithm based on a voltage sensor for a SEPIC converter with a battery load is implemented.

V. Analysis of proposed topology

The Z–source was first introduced for overcoming the limited voltage gain in DC–AC power conversion [17]. The Z–source allows increasing the output voltage by storing the energy in an LC filter then delivering it, feeding the conventional converter with a voltage larger than the input voltage. Another approach for increasing the gain consists in employing diode–capacitor pairs for multiplying the output voltage in a DC−DC converter. Both topologies are arranged in a full-bridge configuration, but the latter idea is taken for realizing a family of converter [10]. The proposed converter for MPP applications is shown in Fig. 4.

The proposed converter is constituted by the combination of a conventional boost converter with a diode-capacitor multiplier for obtaining an additional gain, besides an LC filter for

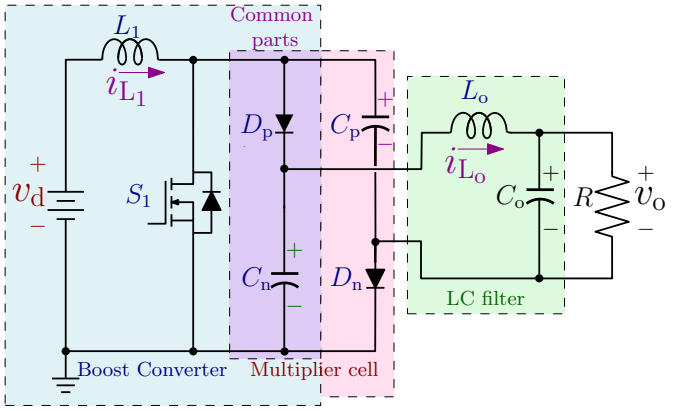

Fig. 4: Proposed topology.

smoothing the output voltage produced by the MPP algorithm and the switching process. Different parts are identified in Fig. 4; it is worth noting that D_P and C_n are shared by the boost converter and the multiplier parts. For the following analysis, the equivalent series resistances of the inductors is also taken into account, represented by $r_{L_{(1,o)}}$, for obtaining a more realistic behaviour.

A. Equivalent circuit states

Since the proposed topology contains only one single power switch, two equivalent circuits are obtained, seen in Fig. 5. Nevertheless, it is always expected to work in the CCM.

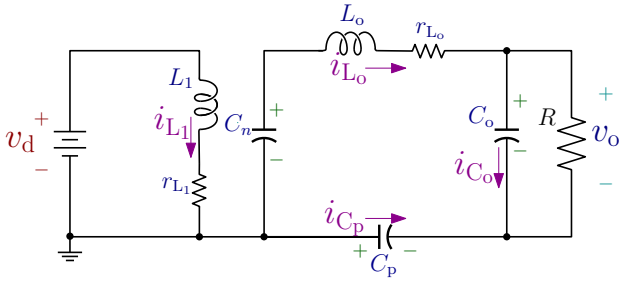

(a) Equivalent circuit corresponding to the active state.

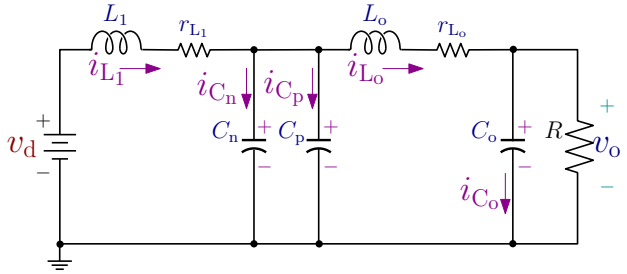

(b) Equivalent circuits corresponding to the inactive state.

Fig. 5: Equivalent circuits for the proposed converter.

1) Active state $0 \leq t \leq DT_s$: For this state, with the commanding signal $q(t) = 1$, the input inductor is connected directly to the input voltage producing an increasing in its current as (1) indicates. Due to C_n belongs to the boost converter stage, its voltage is close to $v_d/(1-D)$ V. The LC

filter is fed by the series connection of C_{p} and C_{n}, providing $2 \cdot v_{\mathrm{d}}/(1-D)$ V. Therefore, the output stage can be seen as a buck converter whose input voltage is twice $v_{\mathrm{d}}/(1-D)$ V, as illustrated in Fig. 5a. During this state, both diodes are reverse-biased, blocking their corresponding capacitor voltages.

$$V_{\mathrm{L}_1} = L_1 \frac{\Delta i_{\mathrm{L}_1}}{\Delta t} = L_1 \frac{\Delta i_{\mathrm{L}_1}}{DTs} = V_{\mathrm{d}} - i_{\mathrm{L}_1} r_{\mathrm{L}_1} \tag{1}$$

2) Inactive state $DT_{\mathrm{s}} < t \leq (1-D)T_{\mathrm{s}}$*:* For this state, with the commanding signal $q(t) = 0$, the equivalent circuit is presented in Fig. 5b. During this state, the power transistor is turned off whereas both diodes are forward-biased, connecting capacitors C_{n} y C_{p} in parallel. As a consequence, the output filter is fed with $v_{\mathrm{d}}/(1-D)$ V. Current through L_1 decreases with a rate given by (2).

$$V_{\mathrm{L}_1} = L_1 \frac{\Delta i_{\mathrm{L}_1}}{(1-D)Ts} = V_{\mathrm{d}} - i_{\mathrm{L}_1} r_{\mathrm{L}_1} - V_{\mathrm{C}_{\mathrm{n}}} \tag{2}$$

B. Output voltage of the proposed converter

As customary in power electronics converter, a lossless analysis is carried out. Averaging the inductor voltage during a switching period and taking into account the current increment (Δi_{L}), the input/output relationship can be obtained.

$$\Delta i_{\mathrm{L}_{(1,\mathrm{o})}}\Big|_{q=0} + \Delta i_{\mathrm{L}_{(1,\mathrm{o})}}\Big|_{q=1} = 0 \tag{3}$$

With the use of (1), (2) and (3) the total voltage gain is:

$$\frac{V_{\mathrm{C_o}}}{V_{\mathrm{d}}} = \frac{V_{\mathrm{C}}}{V_{\mathrm{d}}} \cdot \frac{V_{\mathrm{C_o}}}{V_{\mathrm{C}}} = \frac{(1+D)}{(1-D)} \cdot \frac{1}{1 + \frac{(1+D)^2}{(1-D)^2} r_{\mathrm{L}_1\prime}} \cdot \frac{1}{1 + r_{\mathrm{L}_0\prime}} \tag{4}$$

C. Output voltage of the buck model

Both states can be combined in the model shown in Fig. 6, which resembles a Buck converter whose inductor switches between v_{d} and $2v_{\mathrm{d}}$, in this way the average output voltage can be easily computed.

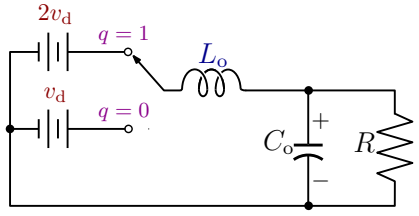

Fig. 6: Buck model.

As assumed in Fig. 6, the average voltage at the load side corresponds to (4) with the parasitic element of inductors set to zero.

VI. Power converter with MPPT controller

The main objective of the MPPT is to match rapidly the impedance Z_{in} with the optimal impedance of PV module at the MPP. The perturbation step size and the perturbation time are two decisive factors. The output power oscillation magnitude depends directly on the step size, the smaller step used is the lower ripple obtained, which is desirable and it gives more sensitiveness to the algorithm. The perturbation time is also crucial since it controls the MPPT response time being able to track the MPP successfully even with temperature and irradiance variations [5].

To select the value of R, the simulation of the PV module without the MPPT controller was analyzed, under constant irradiance and temperature $\left(G = 1,000\ \mathrm{W/m^2}, T = 25°C\right)$. Then using the voltage and current at MPP $(V_{\mathrm{m}}, I_{\mathrm{m}})$ depicted in Fig. 7. Thus the value of R_{m} was calculated from (5) by Ohm's law.

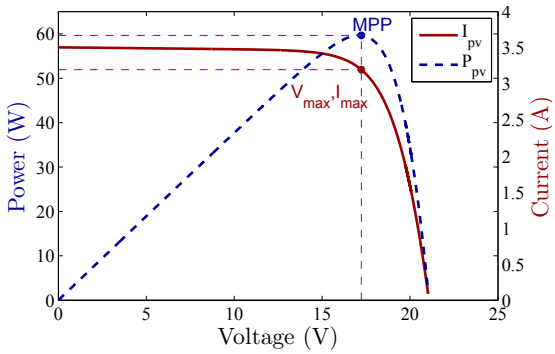

Fig. 7: P-V curve (solid), I-V curve (dashed).

$$R_{\mathrm{m}} = \frac{V_{\mathrm{m}}}{I_{\mathrm{m}}} \tag{5}$$

For maximum power transfer R_{m} must be equal to R.

VII. Simulation results

In order to validate the proposed system, a Matlab Simulink simulation with the parameters given in the Appendix was run.

The closed loop system is shown in Fig. 8 which incorporates the classical P&O algorithm with the power converter. In order for the MPPT controller to calculate the power provided by the PV panel, voltage and current sensors were employed to measure such variables.

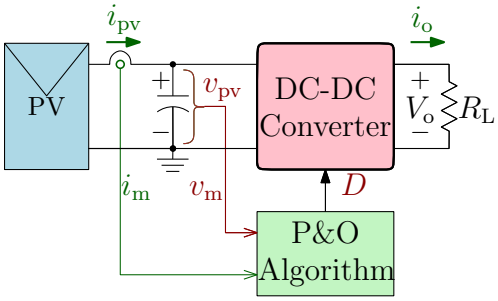

Fig. 8: Closed Loop system.

The Solarex MSX−60 [18] was selected as the PV panel model for the simulation. The module consists of 36 poly-crystalline silicon solar cells electrically configured as two series strings of 18 cells each and provides 60 W as nominal maximum power in STC. The simulation model was based on the one presented in [19].

A comparison between the proposed topology and the conventional boost converter is presented. The switching frequency that controls the proposed converter was set at 28.5 kHz, the PV system was perturbed periodically every 0.2 ms with a duty cycle change Δ_D of $\pm 1\%$. The system was evaluated by applying a step change in the irradiance from 1,000 W/m^2 to 800 W/m^2 with a constant module temperature (T) of 25°C. Results of the simulation are shown in Fig. 9.

As shown in Fig. 9a and Fig. 9b, the converters are capable of tracking the MPP irrespective of increase or decrease in irradiance. The PV power presents small oscillations due to the inherent characteristics of the P&O algorithm. More sophisticated algorithms may be implemented with a better performance however they are out of the scope of this work. For practical purposes, it is considered a low ripple and has no undesirable effects on the power quality.

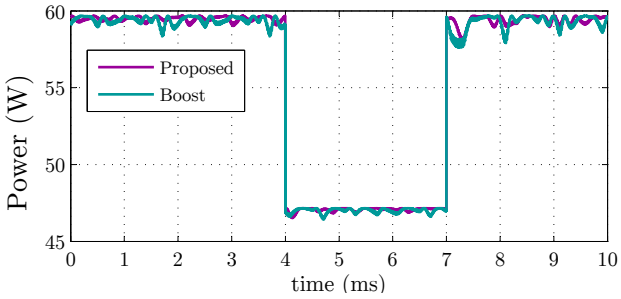

(a) Maximum power extracted under irradiation variations.

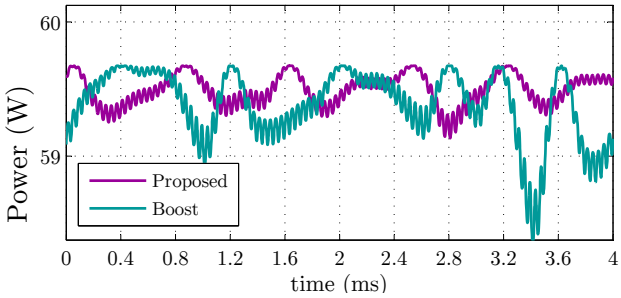

(b) Maximum power extracted (zoomed-in)

Fig. 9: Simulation performance of the proposed system.

Fig. 10 shows the evolution of the duty cycles of both converters under the same disturbance and P&O algorithm parameter conditions. As can be seen, the duty cycle determined by the MPPT operating with the proposed converter is significantly smaller than that of the boost converter. Fig. 11 shows the power extracted versus the PV voltage according to the algorithm when a step change in the irradiance occurs in both converters. It can be observed that the operating point path achieves the maximum value even when a rapid change in irradiance occurs.

VIII. Experimental Results

In this section is presented the behaviour of the output PV power by manipulating the value of Z_{in}. Fig. 12 shows the laboratory prototype used for this experiment. A conventional boost converter was implemented for this study and their

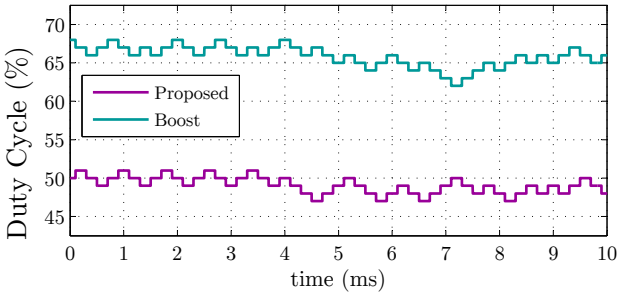

Fig. 10: Simulated waveforms: Duty Cycles at MPP.

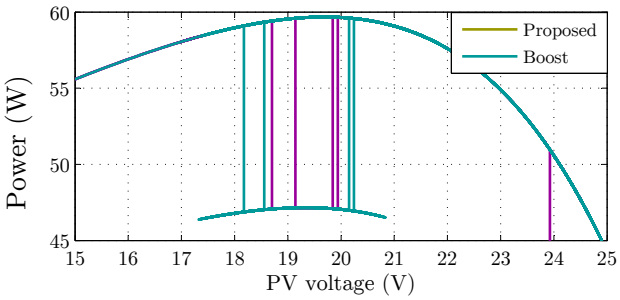

Fig. 11: Power and voltage PV for both converters.

components are listed in Table II. A switching frequency signal of 28.5 kHz with a variable duty cycle from 10% to 87% was applied to the power converter. Additionally, the V_{pv} and i_{pv} produced by a polycrystalline generic PV panel were measured with current and voltage sensors by means the ADC of ATmega328P microcontroller. These signals were captured with a digital scope TPS2024 from Tektronix.

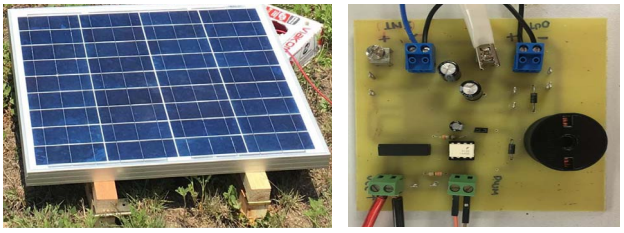

Fig. 12: Prototype photo.

Fig. 13 presents the duty cycles corresponding to the maximum power generated by the PV panel. As presented in Table I it is evident that there is a corresponding value of D for a different R_{L} at which the output power reaches the maximum point. By changing R_{L} to a higher value the suitable D obtained experimentally increases, so that the value of Z_{in} becomes smaller, otherwise Z_{in} gets higher.

IX. Conclusions

In this paper a high step−up DC−DC converter suitable for PV applications was proposed. This converter presents a higher voltage gain than that of a conventional boost converter and it is appropriate for this purpose. A simulation including a P&O MPPT technique was shown to support its effectiveness even under varying irradiance. This paper explains the operating principle of the proposed converter. Unlike the conventional

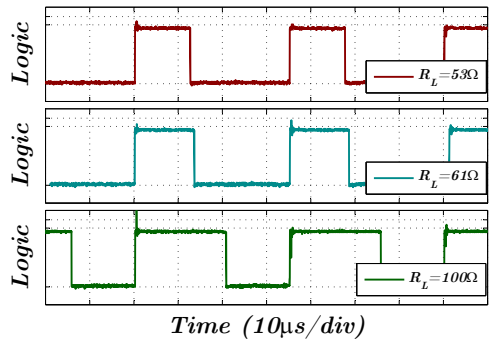

Fig. 13: Experimental waveforms: Duty Cycles at MPP.

boost converter, the suggested topology can extract the maximum power with a relatively low duty cycle. The experimental results evidence the effect of the input impedance in the closed loop system and show the values of duty cycle that the MPPT must provide for given conditions.

ACKNOWLEDGMENT

The authors would like to thank TECNOLÓGICO NACIONAL DE MÉXICO and Instituto Tecnológico de Ciudad Madero for supporting this research under Grant: 6060.17−P.

APPENDIX

TABLE II: Parameters of the various components.

Symbol	Value
Power Components	
Boost Converter	
v_{in}	10 V
L_1	680 μH
C_{n}	200 μF
R	53 Ω, 61 Ω and 100 Ω
Proposed Topology	
v_{in}	10 V
$L_1 = L_{\text{o}}$	44 μH
$C_{\text{p}} = C_{\text{n}} = C_{\text{o}}$	100 μF
R	45 Ω
Devices	
MCU	ATmega328P
S_1	FDD5353
D_1	1N4936G
Gate driver	A3120

REFERENCES

[1] N. Femia, G. Petrone, G. Spagnuolo, and M. Vitelli, "Optimization of perturb and observe maximum power point tracking method," *IEEE Transactions on Power Electronics*, vol. 20, no. 4, pp. 963–973, July 2005.

[2] B. Subudhi and R. Pradhan, "A comparative study on maximum power point tracking techniques for photovoltaic power systems," *IEEE Transactions on Sustainable Energy*, vol. 4, no. 1, pp. 89–98, Jan 2013.

[3] M. A. G. de Brito, L. Galotto, L. P. Sampaio, G. d. A. e Melo, and C. A. Canesin, "Evaluation of the main mppt techniques for photovoltaic applications," *IEEE Transactions on Industrial Electronics*, vol. 60, no. 3, pp. 1156–1167, March 2013.

[4] E. D. Aranda, J. A. G. Galan, M. S. de Cardona, and J. M. A. Marquez, "Measuring the i-v curve of pv generators," *IEEE Industrial Electronics Magazine*, vol. 3, no. 3, pp. 4–14, Sept 2009.

[5] M. Killi and S. Samanta, "Modified perturb and observe mppt algorithm for drift avoidance in photovoltaic systems," *IEEE Transactions on Industrial Electronics*, vol. 62, no. 9, pp. 5549–5559, Sept 2015.

[6] W. Xiao, M. S. E. Moursi, O. Khan, and D. Infield, "Review of grid-tied converter topologies used in photovoltaic systems," *IET Renewable Power Generation*, vol. 10, no. 10, pp. 1543–1551, 2016.

[7] P. M. Garcia-Vite, A. Soriano-Rangel, J. C. Rosas-Caro, and F. Mancilla-David, "A dc-dc converter with quadratic gain and input current ripple cancelation at a selectable duty cycle," *Renewable Energy*, vol. 101, pp. 431 – 436, 2017. [Online]. Available: http://www.sciencedirect.com/science/article

[8] N. Mohan, T. M. Undeland, and W. P. Robbins, *Power Electronics. Converters, Applications and Design*, 3rd ed. John Wiley and Sons, Inc, 2003.

[9] A. P. Bhatnagar and B. R. K. Nema, "Conventional and global maximum power point tracking techniques in photovoltaic applications: A review," *Journal of Renewable and Sustainable Energy*, vol. 5, no. 3, p. 032701, May 2013.

[10] B. Axelrod, Y. Berkovich, A. Shenkman, and G. Golan, "Diode-capacitor voltage multipliers combined with boost-converters: topologies and characteristics," *IET Power Electronics*, vol. 5, no. 6, pp. 873–884, July 2012.

[11] C. C. Hua, Y. H. Fang, and W. T. Chen, "Hybrid maximum power point tracking method with variable step size for photovoltaic systems," *IET Renewable Power Generation*, vol. 10, no. 2, pp. 127–132, 2016.

[12] H. A. Sher, A. F. Murtaza, A. Noman, K. E. Addoweesh, K. Al-Haddad, and M. Chiaberge, "A new sensorless hybrid mppt algorithm based on fractional short-circuit current measurement and p&o mppt," *IEEE Transactions on Sustainable Energy*, vol. 6, no. 4, pp. 1426–1434, Oct 2015.

[13] L. M. Elobaid, A. K. Abdelsalam, and E. E. Zakzouk, "Artificial neural network-based photovoltaic maximum power point tracking techniques: a survey," *IET Renewable Power Generation*, vol. 9, no. 8, pp. 1043–1063, 2015.

[14] D. N. M. Vilathgamuwa and S. Gamini, *Power Electronics for Photovoltaic Power Systems*. Morgan & Claypool, 2015.

[15] E. Koutroulis and K. Kalaitzakis, "Novel battery charging regulation system for photovoltaic applications," *IEE Proceedings - Electric Power Applications*, vol. 151, no. 2, pp. 191–197, Mar 2004.

[16] M. Killi and S. Samanta, "An adaptive voltage-sensor-based mppt for photovoltaic systems with sepic converter including steady-state and drift analysis," *IEEE Transactions on Industrial Electronics*, vol. 62, no. 12, pp. 7609–7619, Dec 2015.

[17] F. Z. Peng, "Z source inverter," *IEEE Transactions on Industry Applications*, vol. 39, no. 2, p. 504510, Mar 2003.

[18] Solarex, *Solarex MSX-60 Manufacturer Specification sheet*, Solarex, Frederick, MD 21703 USA, 1997.

[19] S. Pukhrem, "A photovoltaic panel model in matlab/simulink," *11th students' science conference : Bedlewo*, pp. 115–120, Oct 2013.